

REMOVAL OF NICKEL IONS FROM AQUEOUS SOLUTION ON A STRONG ACID MACRONET RESIN. KINETIC ANALYSIS

Sorinela Daniela CANTEA¹, Eugen PINCOVSCHI², Ana Maria S. OANCEA³

The ion exchange kinetics of H^+/Ni^{2+} on a relatively new hyper-crosslinked styrene-divinylbenzene sulfonated polymer was investigated in order to evaluate the material for removal of nickel ions from wastewaters. The ion exchanger has macro-, meso- and micropores. The ion exchange rate was measured at 298 K in conditions favoring a particle diffusion control using a potentiometric method. The results were modelled with both quasi-homogeneous and bidisperse pore kinetic models. The H^+/Ni^{2+} interdiffusion coefficients obtained with the different kinetic models were compared and discussed. The evaluated H^+ and Ni^{2+} self-diffusion coefficients at 298 K are $2.37 \cdot 10^{-10}$ and $3.75 \cdot 10^{-12} \text{ m}^2 \text{ s}^{-1}$, respectively.

Keywords: ion exchange kinetics; interdiffusion coefficient; nickel(II) ion; macronet resin; sulfonated polystyrenic resins; porous ion exchanger

List of symbols

\bar{D}	effective intraparticle diffusivity; self-diffusion coefficient for isotopic exchange; integral interdiffusion coefficient for mutual ion-exchange ($\text{m}^2 \text{ s}^{-1}$)
\bar{D}_a	effective macropore diffusivity; macropore self-diffusion coefficient for isotopic exchange; macropore integral interdiffusion coefficient for mutual ion-exchange ($\text{m}^2 \text{ s}^{-1}$)
\bar{D}_i	effective micropore diffusivity; micropore self-diffusion coefficient for isotopic exchange; micropore integral interdiffusion coefficient for mutual ion-exchange ($\text{m}^2 \text{ s}^{-1}$)
\bar{e}, e	number of ion equivalents at equilibrium in the resin and solution phases (eq)
F	fractional attainment of equilibrium (dimensionless)
$M_{a\infty}$	macropore uptake at equilibrium (eq/kg)
$M_{i\infty}$	micropore uptake at equilibrium (eq/kg)
n	number of terms in a series
pH_0, pH_∞, pH_t	pH of the external solution at $t = 0$, equilibrium and time t

¹ PhD student, Department of Analytical Chemistry and Environmental Engineering, University POLITEHNICA of Bucharest, Romania, e-mail: cadana@yahoo.com

² Prof., Department of Analytical Chemistry and Environmental Engineering, University POLITEHNICA of Bucharest, Romania

³ Prof., Department of Inorganic Chemistry, Physical Chemistry and Electrochemistry, University POLITEHNICA of Bucharest, Romania

\bar{r}_0	mean radius of the resin swollen beads (m)
\bar{r}_i	microsphere radius (m)
S_n	roots of equation $S_n \cot S_n = 1 + S_n^2/3\omega$
t	time (s)
Greek Symbols	
$\alpha = \bar{D}_i \bar{r}_0^2 / \bar{D}_a \bar{r}_i^2$	dimensionless rate parameter
$\beta / \alpha = 3 M_{i\infty} / M_{a\infty}$	dimensionless equilibrium parameter
α', β'	roots of equation $x^2 + 3\omega x - 3\omega = 0$
$\theta = \bar{D}_a t / \bar{r}_0^2$	dimensionless time
$\tau = \bar{D} t / \bar{r}_0^2$	dimensionless time
$\omega = \bar{e} / e$	dimensionless equilibrium parameter

1. Introduction

Nickel removal from polluted waters arising from a large variety of sources as mining, metallurgy, nickel plating in electronic and automotive industries, rechargeable batteries, used catalysts, contact of water with nickel- or nickel-chromium plated taps is necessary because of its toxic effects. Nickel causes allergies, genetic damage and cancer. The concentration of nickel(II) in drinking water is limited to 0.02 mg/L [1,2].

Ion exchange is a classical procedure for purifying waste aqueous streams and many ion exchangers could be used in an industrial application. The most popular are the functionalized styrene-divinylbenzene (ST-DVB) polymers. A third generation of ST-DVB polymers were obtained [3,4] being hypercrosslinked and having macro-, meso- and a large amount of micropores, which become in the last time commercial products [5], designated as "macronet resins".

The main objective of the present work was to investigate the ion exchange kinetics of H^+/Ni^{2+} on the relative new macronet strong acid cation exchanger Purolite MN500 in order to evaluate this material for nickel removal from wastewaters by ion exchange. The specific objectives were: a) experimental determination of H^+/Ni^{2+} ion exchange rate in different conditions using a potentiometric method; b) modeling the data with different kinetic models and calculation of H^+/Ni^{2+} interdiffusion coefficients. Two classes of kinetic models were considered: i) models assuming the ion exchanger as a quasi-homogeneous phase (QHRP); and ii) a bidisperse pore kinetic model (BDM).

Previous investigations on H^+/Ni^{2+} ion exchange kinetics were preformed for gel and macroporous sulfonated resins [1,6], and to our knowledge no data were reported for hypercrosslinked cation exchangers.

2. Kinetic models

Quasi-homogeneous resin phase kinetic models (QHRP) for particle diffusion control. The ion exchange process is a diffusion phenomenon and was described using the equations derived for isotopic exchange [7] for two limiting mechanisms when: a) the ion interdiffusion in the particle of the ion exchanger is the rate limiting step, the ion exchanger being considered as a quasi-homogeneous phase, and b) the ion interdiffusion in the Nernst layer is the rate limiting step. In the isotopic exchange kinetic model the influence of the electrical forces on the ion interdiffusion was not taken into account, and the self-diffusion coefficient of an ion is a constant. The H^+/Ni^{2+} ion exchange rate was measured in conditions favoring a particle diffusion controlled mechanism, so that the following treatment refers to this case. The exchanged fraction at time t is given by the analytical solution of the Fick's second law for infinite solution volume (ISV) boundary condition (F-ISV) [7]:

$$F(t) = 1 - \frac{6}{\pi^2} \sum_{n=1}^{\infty} \frac{1}{n^2} \exp(-n^2 \pi^2 \tau) \quad (1)$$

Reichenberg proposed a simplified equation for ISV for $F < 0.85$ [8]:

$$F(t) = \frac{6}{\pi^{3/2}} (\pi^2 \tau)^{1/2} - \frac{3}{\pi^2} (\pi^2 \tau) \quad (2)$$

The half-time of the ion exchange was derived [7] from equation 1 and it is:

$$t_{1/2} = 0.030 \frac{\bar{r}_0^2}{D} \quad (3)$$

The analytical solution of the Fick's second law at finite solution volume (F-FSV) is [7]:

$$F(t) = 1 - \frac{2}{3\omega} \sum_{n=1}^{\infty} \frac{\exp(-S_n^2 \tau)}{1 + S_n^2 / 9\omega(\omega + 1)} \quad (4)$$

The slow convergence of the series in equation 3 was surpassed by Paterson who proposed an approximation for FSV when the dimensionless time $\tau < 0.1$ [7]:

$$F(t) = \frac{\omega + 1}{\omega} \left(1 - \frac{1}{\alpha' - \beta'} [\alpha' \exp(\alpha'^2 \tau) (1 + \operatorname{erf} \alpha' \tau^{1/2}) - \beta' \exp(\beta'^2 \tau) (1 + \operatorname{erf} \beta' \tau^{1/2})] \right) \quad (5)$$

Bidisperse pore kinetic model (BDM). Ruckenstein *et al.* developed a kinetic model for sorption of species by diffusion into a porous solid with macro- and micropores at ISV with constant diffusion coefficients [9]. The particle of the porous ion exchanger is a sphere of mean radius \bar{r}_0 and contains microspheres with mean radius \bar{r}_i . The microspheres contain micropores and the spaces between the microspheres are macropores. Two hypotheses were considered: a) competitive diffusion in macro- and micropores (BDM-CD); b) a limiting case for a step-by-step diffusion in macro- and the micropores (BDM-LC). The exchanged fraction over time is given in BDM-CD by [9]:

$$F = \frac{M_t}{M_\infty} = \frac{\sum_{k=1}^{\infty} \sum_{q=1}^{\infty} \frac{k^2 [1 - \exp(-\alpha \xi_{qk}^2 \theta)]}{\xi_{qk}^4 \left[\frac{\alpha}{\beta} + 1 + \cot^2 \xi_{qk} - \left(1 - \frac{k^2 \pi^2}{\beta}\right) \frac{1}{\xi_{qk}^2} \right]}}{\sum_{k=1}^{\infty} \sum_{q=1}^{\infty} \frac{k^2}{\xi_{qk}^4 \left[\frac{\alpha}{\beta} + 1 + \cot^2 \xi_{qk} - \left(1 - \frac{k^2 \pi^2}{\beta}\right) \frac{1}{\xi_{qk}^2} \right]}} \quad (6)$$

and for BDM-LC by [9]:

$$F = \frac{M_t}{M_\infty} = \frac{\left[1 - \frac{6}{\pi^2} \sum_{n=1}^{\infty} \frac{1}{n^2} \exp(-n^2 \pi^2 \theta) \right] + \frac{1}{3} (\beta/\alpha) \left[1 - \frac{6}{\pi^2} \sum_{n=1}^{\infty} \frac{1}{n^2} \exp(-n^2 \pi^2 \alpha \theta) \right]}{1 + \frac{1}{3} (\beta/\alpha)} \quad (7)$$

The parameters $\alpha = \bar{D}_i \bar{r}_0^2 / \bar{D}_a \bar{r}_i^2$ and $\beta/\alpha = 3 M_\infty / M_\infty$ represent the ratio of the rates of sorption in micropores and macropores, and the ratio of the amount of ion sorbed in micropores and macropores at equilibrium, respectively. The correspondence between β/α and M_∞ / M_∞ is given in Table 1.

In real ion exchange processes, the self-diffusion coefficient is not a constant and varies with the ionic composition of the ion exchanger, due to the influence of the electrical forces on the ionic flux [7]. Using equations 1-7 for computing the interdiffusion coefficients of a mutual exchange at an exchanged fraction F implies the assumption that the interdiffusion coefficient is a constant for each 0- F interval, and it is called „integral interdiffusion coefficient” [10-13].

Table 1
Correspondence between the parameter β/α and the ratio of the resin loading at equilibrium in micro and macropores, $M_{i\infty}/M_{a\infty}$

β/α	0.003	0.01	0.03	0.05	0.1	0.3	1	3	6	30	300
$M_{i\infty}/M_{a\infty}$	1/1000	1/300	1/100	1/60	1/30	1/10	1/3	1/1	2/1	10/1	100/1

3. Experimental

The commercial Purolite MN500 strong acid macronet resin was air-dried and sieved in four size fractions. Each fraction was purified in a column in three cycles of successive treatments with an excess of 1 M HCl, demineralized water (with specific conductivity of $\sim 0.05 \mu\text{S cm}^{-1}$) and 1 M NaOH solutions. The final treatment was with 300% excess 1 M HCl and rinsed until the effluent had less than $1 \mu\text{S cm}^{-1}$. The resin was air dried and kept in a desiccator over a saturated solution of NaCl, to become saturated with water vapor until reaching a constant weight. The properties of the resin given by the manufacturer [5], determined in this work and reported in a previous paper [15] are given in Table 2.

Table 2
Properties of the ion exchanger Purolite MN500 and the experimental conditions

Resin properties	
matrix	styrene-divinylbenzene, macronet; hyper-reticulated*
functional group	$-\text{SO}_3\text{H}^*$
weight capacity (Na^+ form) (eq/kg)	2.52
specific gravity / (g cm^{-3})	1.52**
moisture (%) (H^+ form)	57.4
surface area / ($\text{m}^2 \text{g}^{-1}$) BET _{N2}	330**
pore volume (mL g^{-1})	0.64**
d50 / (nm) meso- and macropores	150**
d50 / (nm) micropores	1.5*
Experimental conditions	
initial concentration of $\text{Ni}(\text{NO}_3)_2$ in the kinetic run / M	0.45
stirring speed / (min^{-1})	500; 600
temperature / (K)	298

*[5]; **mean values for different size fractions given in reference [15]

The $\text{H}^+/\text{Ni}^{2+}$ ion exchange rate on macronet MN500 resin was measured in batch experiments by monitoring potentiometrically the outgoing proton with WTW inoLab pH/cond 740 meter. The procedure was described in detail in previous papers [6,11-14]. The experimental conditions are reported in Table 2. The interference of the electrolyte desorption during the kinetic runs was

investigated and was negligible. The mean values of the swollen resin particles for different size fractions were measured microscopically in H^+ and Ni^{2+} form, and are given in Table 3, as a mean of 50 measurements. The confidence limits correspond to 99% probability and a Student distribution.

Table 3

Mean radius of the swollen resin particles of MN500 resin		
Size fraction sieve diameter/(\mu m)	H^+ form $\cdot 10^3$ (m)	Ni^{2+} form $\cdot 10^3$ (m)
[-710+630]	0.338 ± 0.020	0.372 ± 0.011
[-630+500]	0.283 ± 0.010	0.297 ± 0.015
[-500+400]	0.219 ± 0.009	0.227 ± 0.016
[-400+300]	0.168 ± 0.009	0.198 ± 0.010

4. Results and discussion

The ion exchange kinetic curves were measured in experimental conditions favoring a particle diffusion controlled mechanism, namely in concentrated external solutions (~ 1 eq/L) under efficient stirring. Moreover, the selected conditions are in agreement also with the infinite solution volume boundary conditions, because the ratio between the solution volume and the resin mass was equal to 100, and the ratio between the amount of ions in the resin phase and in the solution phase was less than 0.03. The exchanged fraction F was obtained from the pH variation in the external solution with equation:

$$F = \frac{10^{-pH_t} - 10^{-pH_0}}{10^{-pH_\infty} - 10^{-pH_0}} \quad (8)$$

This equation is valid when the ionic strength is constant during the ion exchange process. In the selected experimental conditions, the ionic strength was 1.35 M and varied during the H^+/Ni^{2+} ion exchange with maximum 1%, and the variation of the proton activity coefficient was negligible.

Figure 1 gives the kinetic curves obtained for different size fractions of the macronet resin at constant stirring speed (500 min^{-1}) and Figure 2 the influence of the stirring on the H^+/Ni^{2+} ion exchange process. A good reproducibility of the kinetic data can be observed. The increase of the ion exchange rate with the decrease of the size of the resin particles, and the lack of influence of the stirring speed on the ion exchange rate support a mechanism controlled by the particle diffusion step. Moreover, the linear dependence of the half-time with the square of the radius of the resin beads, as can be seen in Figure 3, is also an argument supporting this mechanism. The H^+/Ni^{2+} integral interdiffusion coefficient at half

exchange evaluated using equation 3 and the slope of the plot in Figure 3 was $1.01 \cdot 10^{-10} \text{ m}^2 \text{ s}^{-1}$.

Several kinetic equations were fitted to the experimental curves in order to obtain an empirical equation describing the ion exchange process. The results for the best fit are given in Table 4.

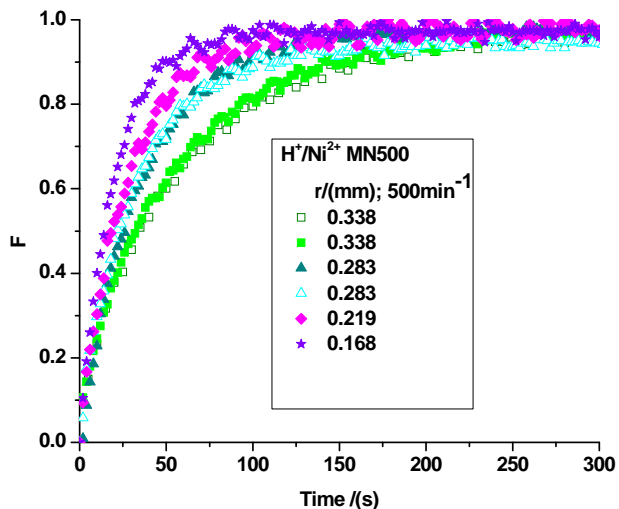


Fig. 1. Variation of the fractional attainment of equilibrium over time for $\text{H}^+/\text{Ni}^{2+}$ ion exchange process on different size fractions of macronet strong acid resin MN500; 298 K; 0.90 eq/L $\text{Ni}(\text{NO}_3)_2$.

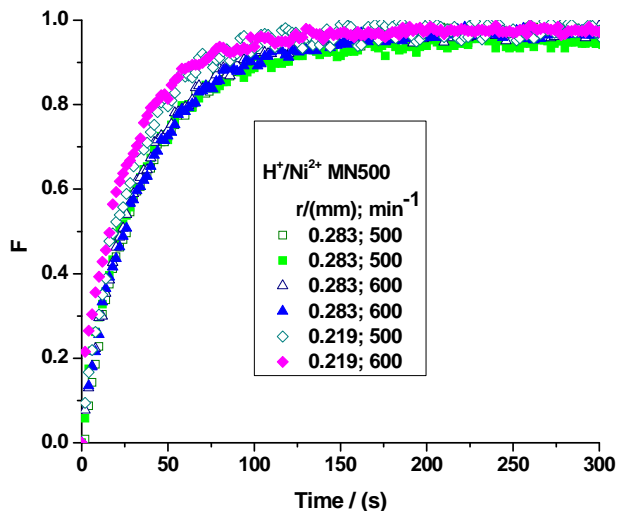


Fig. 2. Influence of the stirring speed on $\text{H}^+/\text{Ni}^{2+}$ ion exchange process on macronet strong acid resin MN500; 298 K; two size fractions; 0.90 eq/L $\text{Ni}(\text{NO}_3)_2$.

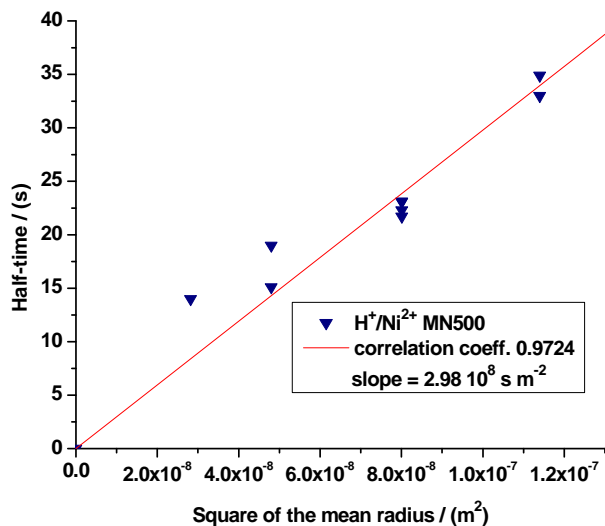


Fig. 3. Linear dependence of the half-time on the square of the radius of the swollen resin beads for $\text{H}^+/\text{Ni}^{2+}$ ion exchange process on macronet MN500 resin; 298 K; 0.90 eq/L $\text{Ni}(\text{NO}_3)_2$.

Table 4
Coefficients of the empirical kinetic equation for H^+/Ni^+ ion exchange process on MN500 resin; 298 K; 0.45 M $\text{Ni}(\text{NO}_3)_2$; 95% confidence limits; parameter of goodness of fit: r-square, and F-statistics

$$F = a(1 - \exp(-bt)) + c(1 - 1/(1 + cdt))$$

$\bar{r}_0 \cdot 10^3$ (m)	No. exp. pcts.	<i>a</i>	<i>b</i>	<i>c</i>	<i>d</i>	r-square	F-statistics
0.338	1715	$0.740 \pm$ 0.043	$0.01522 \pm$ 0.00040	$0.235 \pm$ 0.045	$0.60 \pm$ 0.36	0.9919	13922
		$0.736 \pm$ 0.024	$0.01600 \pm$ 0.00020	$0.235 \pm$ 0.025	$0.67 \pm$ 0.22	0.9970	49554
0.283	3342	$0.7908 \pm$ 0.0174	$0.02700 \pm$ 0.00050	$0.187 \pm$ 0.018	$0.57 \pm$ 0.12	0.9890	50363
		$0.737 \pm$ 0.031	$0.02815 \pm$ 0.00074	$0.215 \pm$ 0.032	$0.55 \pm$ 0.20	0.9927	23985
0.283	2544	$0.784 \pm$ 0.019	$0.02950 \pm$ 0.00070	$0.193 \pm$ 0.019	$0.31 \pm$ 0.04	0.9919	51986
		$0.733 \pm$ 0.019	$0.02550 \pm$ 0.00040	$0.243 \pm$ 0.020	$0.65 \pm$ 0.15	0.9934	52657
0.219	238	$0.800 \pm$ 0.064	$0.0352 \pm$ 0.0019	$0.196 \pm$ 0.075	$0.34 \pm$ 0.28	0.9983	23277
		$0.785 \pm$ 0.018	$0.03390 \pm$ 0.00050	$0.196 \pm$ 0.018	$6.20 \pm$ 3.44	0.9945	38673
0.168	848	$0.955 \pm$ 0.042	$0.0504 \pm$ 0.0012	$0.020 \pm$ 0.043	$48 \pm$ 489	0.9902	14194

The empirical kinetic equation was used for obtaining interpolated F vs. t files for $0.01 < F < 0.99$. The calculation of the interdiffusion coefficients with different kinetic models was done using these files. Four computer programs developed and reported previously [6,11-13] were utilized for computations. Figure 4 gives the $\text{H}^+/\text{Ni}^{2+}$ integral interdiffusion coefficients on the strong acid macronet resin MN500 for the same size fraction obtained with QHRP kinetic models at ISV and FSV described by the equations 1, 2, 4 and 5.

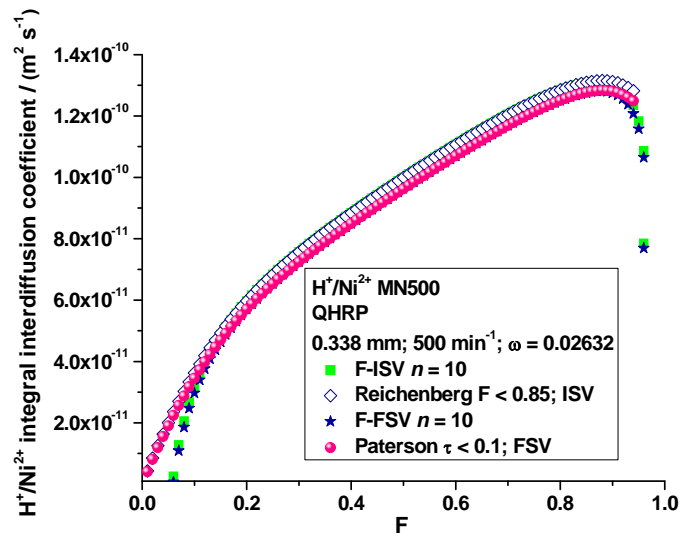


Fig. 4. Comparison of the $\text{H}^+/\text{Ni}^{2+}$ integral interdiffusion coefficients on the strong acid macronet resin MN500 obtained with QHRP kinetic models for particle diffusion control; 298 K.

Table 5
 $\text{H}^+/\text{Ni}^{2+}$ integral interdiffusion coefficients on strong acid macronet resin MN500 for different size fractions obtained with Paterson QHRP-FSV kinetic model; 298 K

Size fraction sieve aperture / (μm)	$\bar{r}_0 \cdot 10^3$ (m)	$\bar{D} \cdot 10^{10}$ $F = 0.01$ ($\text{m}^2 \text{s}^{-1}$)	$\bar{D} \cdot 10^{10}$ $F = 0.50$ ($\text{m}^2 \text{s}^{-1}$)	$\bar{D} \max \cdot 10^{10}$ ($\text{m}^2 \text{s}^{-1}$)
+630	0.338	0.0411	0.963	2.39
		0.0454	1.02	2.41
+500	0.283	0.0273	1.02	2.85
		0.0305	1.06	1.42
		0.0230	1.02	2.65
+425	0.219	0.0376	1.09	2.73
		0.0164	0.745	2.39
		0.101	0.936	2.52
+300	0.168	0.0148	0.598	1.95
Mean value*		0.0375 ± 0.024	0.94 ± 0.15	2.37 ± 0.41

*99% confidence limits for Student distribution

In Table 5 the numerical values of these coefficients are given at three exchanged fractions for all investigated size fractions computed with QHRP-FSV equation 5. The comparison of the results in Figure 4 shows that: a) the series in equations 1 and 4 are not convergent for 10 terms for $F < 0.1$; b) the QHRP-ISV models gives results in good agreement with the rigorous QHRP-FSV models, when the ratio ω is less than 0.03; c) the Reichenberg approximation (equation 2) gives practically the same results for ISV as the rigorous equation 1 with 10 terms in the series (F-ISV). Moreover, with this equation the interdiffusion coefficients can be computed when the series in equation 1 is not convergent; d) the Paterson approximation for $\tau < 0.1$ (equation 5) gives the same results as the rigorous equation 4 with $n = 10$ (QHRP-FSV) and avoid the problem of series convergence.

The “minority rule” of Helfferich [7] establishes that the interdiffusion coefficient tends to the self-diffusion coefficient of the ion in trace concentration in the resin phase. Therefore the H^+/Ni^{2+} interdiffusion coefficient at $F = 0.01$ given in Table 4 ($3.75 \cdot 10^{-12} \text{ m}^2 \text{ s}^{-1}$) evaluates the Ni^{2+} self-diffusion coefficient in the strong acid macronet resin MN500 and the maximum value of the interdiffusion coefficient obtained at high F values ($2.37 \cdot 10^{-10} \text{ m}^2 \text{ s}^{-1}$) evaluates the H^+ self-diffusion coefficient in the macronet resin. The proton and Ni^{2+} self-diffusion coefficients in dilute aqueous solution at 298 K are $9.311 \cdot 10^{-9} \text{ m}^2 \text{ s}^{-1}$ and $0.661 \cdot 10^{-9} \text{ m}^2 \text{ s}^{-1}$ respectively [16], and the proton self-diffusion coefficients in a phenol-formaldehyde resin was reported as $2.4 \cdot 10^{-9} \text{ m}^2 \text{ s}^{-1}$ [17,18]. Comparing the obtained values with the corresponding values in dilute aqueous solution it can be observed that the matrix of the macronet resin produces a notable retardation of ion diffusion. The Ni^{2+} self-diffusion coefficient decreases around 175 times as compared to water and the proton self-diffusion coefficient decreases around 40 times as compared to water and 10 times as compared to phenol-formaldehyde resin.

The QHRP kinetic models are only a rough approximation for ion exchange kinetics in porous resins. Consequently, the experimental data for H^+/Ni^{2+} ion exchange kinetics on the macronet resin MN500 were modeled also with a bidisperse pore kinetic model. The macronet resin has macro-, meso- and micropores [5,15]. In the first approximation we can consider the real macro- and mesopores as “macropores”, and thus the resin having a bidisperse pore structure. The distribution of the sulfonic acid groups between these pores is not known, and it is not known also if the ion exchange process takes place only in macropores or in both macro- and micropores. The considered kinetic model [9] makes two theoretical hypotheses. One assumption considered that the ion exchange process occurs in two successive stages, in the first stage only in macropores until the equilibrium is achieved and then in the second stage in the micropores. This is valid for parameter $\alpha = 0.001$. The equation 7 gives the variation of the exchanged

fraction over time for this case (BDM-LC). Solving this equation numerically with a computer program [11] the H^+/Ni^{2+} macropores integral interdiffusion coefficients were computed for hypothetical β/α values and the results are given in Figure 5. It must be noted that the series in equation 7 are not convergent for $n = 10$ and $F < 0.1$.

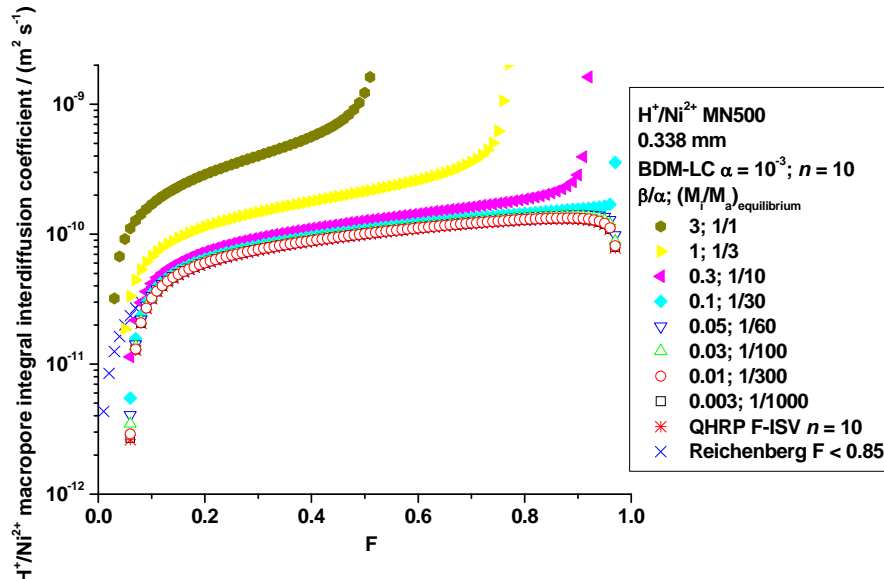


Fig. 5. Macropore integral interdiffusion coefficients of H^+/Ni^{2+} on the strong acid macronet MN500 resin obtained with the limiting case of the bidisperse pore kinetic model for different values of β/α parameter; 298 K.

The other assumption done in the bidisperse pore model was a competitive interdiffusion (parallel diffusion) of ions in macro- and in micropores described by equation 6 (BDM-CD). Two values of the parameter α were taken into account in this work, $\alpha = 0.1$ and $\alpha = 1$. For $\alpha = 0.1$ the ion exchange process is supposed to be ten times faster in macropores than in micropores, and for $\alpha = 1$ the diffusional process is supposed to occur with the same rate in macropores and micropores. The H^+/Ni^{2+} macropore integral interdiffusion coefficients were computed with a computer program [13] for different values of β/α parameter and are given in Figures 6 and 7. Table 6 contains the evaluated self-diffusion coefficients in macropore $\bar{D}_{F=0.01} \rightarrow \bar{D}_{Ni^{2+}}$ and $\bar{D}_{max} \rightarrow \bar{D}_{H^+}$ for different α and β/α .

The obtained macropore interdiffusion coefficients were compared with the self-diffusion coefficients of proton in dilute aqueous solution. All coefficients greater than $9.311 \cdot 10^{-9} \text{ m}^2 \text{ s}^{-1}$ have no physical meaning and were disregarded,

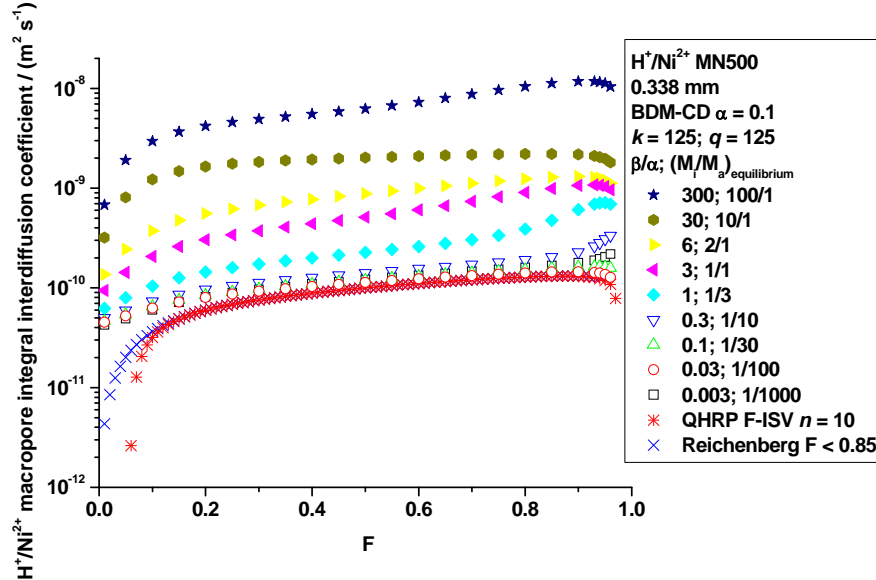


Fig. 6. Macropore integral interdiffusion coefficients of $\text{H}^+/\text{Ni}^{2+}$ on the strong acid macronet MN500 resin obtained with the bidisperse pore kinetic model for competitive diffusion for $\alpha = 0.1$ and different values of β/α parameter; 298 K.

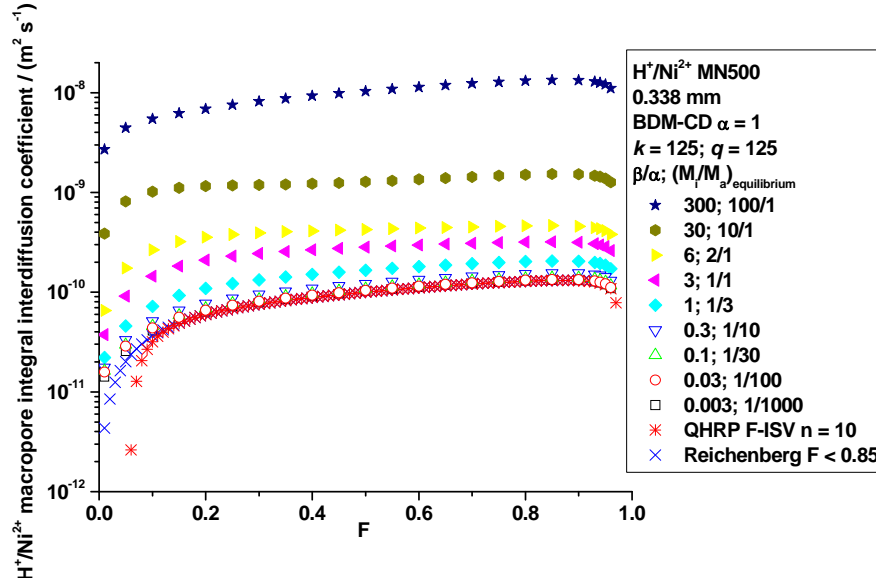


Fig. 7. Macropore integral interdiffusion coefficients of $\text{H}^+/\text{Ni}^{2+}$ on the strong acid macronet MN500 resin obtained with the bidisperse pore kinetic model for competitive diffusion for $\alpha = 1$ and different values of β/α parameter; 298 K.

together with the corresponding values of the parameters α and β/α . The analysis of the data revealed the highest values of β/α and $M_{\infty}/M_{\alpha\infty}$ parameters for a given α parameter which still have physical meaning. The most plausible parameters are collected in Table 7 together with the corresponding interdiffusion coefficients. It must be noted that:

- ❖ if we assume a step-by-step mechanism for H^+/Ni^{2+} ion exchange in the macropores and the micropores of the macronet resin, than the ratio of the micropores and macropores uptake at equilibrium is 1/30, namely to one sulfonic group bound on the micropores walls, 30 groups are bound on the macropores walls;

Table 6
Evaluated macropore self-diffusion coefficients on strong acid macronet resin MN500 obtained with BDM kinetic model; 298 K; 0.338 mm

α	β/α	$\bar{D} \cdot 10^{10}$ $F = 0.01$ ($m^2 s^{-1}$)	$\bar{D} \cdot 10^{10}$ $F = 0.50$ ($m^2 s^{-1}$)	$\bar{D}_{\max} \cdot 10^{10}$ ($m^2 s^{-1}$)
0.001 BDM-LC	0.003		1.00	1.32
	0.01		1.00	1.33
	0.03		1.03	1.37
	0.05		1.04	1.42
	0.1		1.09	1.70
	0.3		1.27	69.0*
	1		2.13	95.4*
	3		12.2*	92.7*
0.1 DBM-CD	0.003	0.425	1.22	2.18
	0.03	0.454	1.13	1.45
	0.1	0.466	1.20	1.63
	0.3	0.500	1.41	3.35
	1	0.623	2.27	7.16
	3	0.944	5.11	10.7
	6	0.137	8.78	13.0
	30	3.19	20.2	22.0
	300	6.79	62.3*	96.0*
1 BDM-CD	0.003	0.142	1.02	1.32
	0.03	0.158	1.04	1.34
	0.1	0.163	1.09	1.40
	0.3	0.175	1.21	1.55
	1	0.222	1.66	2.05
	3	0.373	2.83	3.19
	6	0.653	4.26	4.63
	30	3.86	12.7	15.3
	300	26.9*	104*	133*

*meaningless; $\bar{D}_{F=0.01} \rightarrow \bar{D}_{Ni^{2+}}$; $\bar{D}_{\max} \rightarrow \bar{D}_{H^+}$

- ❖ if we assume the hypothesis of competitive diffusion in macro- and micropores, and a process in macropores 10 times faster than in micropores, the maximum ratio of the number of sulfonic groups existing in micropores and macropores is 2/1;
- ❖ if the mechanism of the ion exchange process is a competitive diffusion in macro- and micropores with the same rate, the conclusion is that to ten functional groups bound in micropores one functional group is bound in macropores (maximum ratio);
- ❖ the H^+/Ni^{2+} integral interdiffusion coefficients at half-exchange obtained with the quasi-homogeneous resin phase kinetic model Paterson $\tau < 0.1$ is in very good agreement with the value obtained from the half-time variation with the square of the resin particles, and with the macropore integral interdiffusion coefficients obtained for a step-by-step diffusion in macropores and micropores, when most of the functional groups exist in macropores (1/30);
- ❖ the Ni^{2+} ion can penetrate the micropores of the macronet resin with a diameter of 1.5 nm [5], because the radius of the hydrated ion is 4.04 Å [19] and the crystal radius is 0.70 Å [19]; the crystal radius depends on the coordination number (CN) and was reported as: 0.69 (CN 4), 0.63 (CN 4 SQ); 0.77 (CN 5); 0.83 (CN 6) [20];
- ❖ if the functional groups are bound mostly in micropores than in macropores, the Ni^{2+} self diffusion coefficient in macropores obtained with BDM is higher in comparison with the value obtained with quasi-homogeneous resin phase kinetic models, and increases with the increased number of sulfonic groups bound in micropores, but remains lower than in dilute aqueous solution, proving a retardation effect caused by the macronet matrix of the resin (see Table7);

Table 7

Comparison of H^+/Ni^{2+} integral interdiffusion coefficients on strong acid macronet resin MN500 obtained with different kinetic models: 0.228 mmol, 208 K

MN500 obtained with different kinetic models; 0.338 mm; 298 K						
Kinetic model	α	β/α	$M_{i\infty}/M_{a\infty}$	$\bar{D}_{F=0.01}$ *	$\bar{D}_{F=0.5}$	\bar{D}_{\max} **
				$\cdot 10^{10} \text{ m}^2 \text{ s}^{-1}$	$\cdot 10^{10} \text{ m}^2 \text{ s}^{-1}$	$\cdot 10^{10} \text{ m}^2 \text{ s}^{-1}$
BDM-LC	0.001	0.1	1/30		1.09	1.7
BDM-CD	0.1	6	2/1	0.14	8.78	13
BDM-CD	1	30	10/1	3.9	12.7	15
Paterson $\tau <$				0.0411	0.963	2.39
0.1				0.0454	1.02	2.41
$t_{1/2}$ vs. \bar{r}_0^2					1.01	
$D_{H^+}^{aq} = 9.311 \cdot 10^{-9} \text{ m}^2 \text{ s}^{-1}$; $\bar{D}_{H^+} = 2.4 \cdot 10^{-9} \text{ m}^2 \text{ s}^{-1}$; $D_{Ni^{2+}}^{aq} = 0.661 \cdot 10^{-9} \text{ m}^2 \text{ s}^{-1}$						
$* \bar{D}_{F=0.01} \rightarrow \bar{D}_{Ni^{2+}}$; $** \bar{D}_{\max} \rightarrow \bar{D}_{H^+}$						

- ❖ the same retardation effect is observed for H^+ self-diffusion coefficient in macropores evaluated with BDM-CD in comparison with the value reported in dilute aqueous solution and in phenol-formaldehyde resin (see Table 7).

The conversion of the macronet resin from H^+ form to Ni^{2+} form was evaluated from the pH measured in a batch reactor in the external solution during the kinetic run and after 24 hours and 14 weeks respectively and the results are given in Figure 8. The conversion was calculated as the ratio between the loading of the resin and the total ion exchange capacity (see Table 2), without correction of the proton activity coefficient. It is interesting to observe that during the kinetic run a minimum pH was obtained (H^+ was the outgoing ion) and a light hydrolysis occurred during 24 hours especially for smaller size fractions, but for a longer time the Ni^{2+} ion entered again in the resin phase. The conversion decreases with the size fraction. The increase of the conversion after 14 weeks is of 5-10%, depending of the size fraction, but remains lower than 100%, supporting the conclusion that Ni^{2+} cannot penetrate in some small pores of the macronet resin.

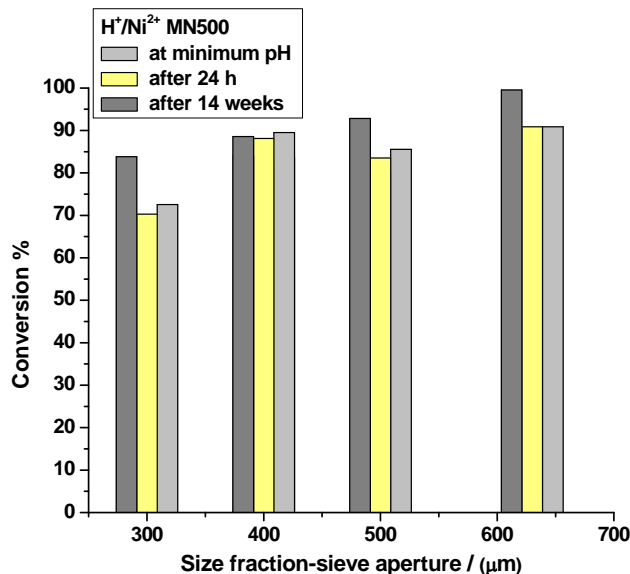


Fig. 8. Conversion of H^+/Ni^{2+} ion exchange on a strong acid macronet resin MN500 in batch experiments; 0.90 eq/L $Ni(NO_3)_2$ solution; (solution volume/resin mass) = 100; 298 K.

5. Conclusions

A relatively new commercial resin was evaluated from kinetic point of view for Ni^{2+} removal from wastewaters. This resin is a third generation of sulfonated styrene-divinylbenzene polymers hyper-reticulated, containing macro-, meso- and micropores. The $\text{H}^+/\text{Ni}^{2+}$ ion exchange rate was measured at 298 K using a potentiometric method in conditions favoring an ion exchange mechanism controlled by the particle diffusion step. The data were modeled with quasi-homogeneous resin phase kinetic models, but also with a bidisperse pore kinetic model. The evaluated H^+ and Ni^{2+} self-diffusion coefficients in the strong acid macronet resin with quasi-homogeneous models were of $2.37 \cdot 10^{-10}$ and $3.75 \cdot 10^{-12}$ $\text{m}^2 \text{ s}^{-1}$ respectively. Within the bidisperse pore kinetic model, three cases were considered: a) the ion exchange process is a step-by-step interdiffusion of ions in macropores and micropores (the process in macropores is thousand times faster than in micropores); b) the ion interdiffusion takes place in parallel in macro- and micropores, ten times faster in macropores than in micropores; c) the ion exchange occurs with the same rate in parallel in macropores and micropores. The $\text{H}^+/\text{Ni}^{2+}$ macropore integral interdiffusion coefficients on the macronet resin MN500 cannot be higher than the proton diffusivity in dilute aqueous solution, thus the ratio between the functional groups bound in micropores and macropores cannot exceed a limiting value. If the ion exchange is a step-by-step diffusion, this limiting ratio between the sulfonic groups existing in micropores and macropores of the macronet resin should be 1/30. If the ion exchange process is a competitive diffusion ten times faster in macropores than in micropores, the limiting ratio between the sulfonic groups bound in micropores and macropores should be 2/1. In the last case, if the ion exchange process is a competitive interdiffusion with equal rate in macropores and micropores, the ratio between the sulfonic groups in micropores and macropores should be maximum 10/1.

Acknowledgements:

The authors acknowledge Purolite International Ltd. for supplying the resin.

R E F E R E N C E S

- [1] Guidelines for Drinking-water Quality, vol. 1, WHO, Geneva **2004**, pp. 416
- [2] *M. Radulescu, M. Cox and A.M.S. Oancea*, Evaluation of a Bidisperse Pore Model for Ion Exchange Kinetics in Porous Media, *Solvent Extr. Ion. Exch.* **30**, 2012, pp. 372-379
- [3] *M.P. Tsyurupa, V.A. Davankov*, Hypercrosslinked polymers: basic principle of preparing a new class of polymeric materials, *React. Funct. Polym.*, **53**, 2002, pp. 193-203
- [4] *M.P. Tsyurupa, V.A. Davankov*, Porous structure of hypercrosslinked polystyrene: State-of-the-art min-review, *React. Funct. Polym.*, **66**, 2006, p 768-779
- [5] *The Purolite Company*, Purolite Technical Bulletin, Hypersol-Macronet Sorbent Resin; Purolite Company, Bala Cynwyd, PA, 1999
- [6] *A.M.S. Oancea, E. Pincovschi, D. Oancea*, Proton/Nickel(II) Interdiffusion Coefficients on Strong Acid Resins, *Solvent Extr. Ion. Exch.* **18**, 2000, pp. 981-1000
- [7] *F. Helfferich*, Ion Exchange, Dover Publication, Inc., New York, chapter 6, pp. 250-322
- [8] *D. Reichenberg*, Properties of Ion-exchange Resins in Relation to their Structure. III. Kinetics of Exchange, *J. Am. Chem. Soc.* **75**, 1953, pp. 589-597
- [9] *E. Ruckenstein, A.S. Vaidyanathan, G.R. Youngquist*, Sorption by solids with bidisperse pore structures, *Chem. Eng. Sci.*, **26**, 1971, 1305-1318
- [10] *T. Zuyi, Z. Aimin, T. Wengong, X. Rong, C. Xingqu*, Studies on Ion Exchange Equilibria and Kinetics. I. Na^+ - H^+ Cation Exchange Equilibrium and Kinetics, *J. Radioanal. Nucl. Chem.* **116**, 1987, pp. 35-47
- [11] *A.M.S. Oancea, E. Pincovschi, D. Oancea, M. Cox*, Kinetic Analysis of Zn(II) removal from Water on Strong Acid Macroreticular Resin Using a Limiting Bidisperse Pore Model, *Hydrometallurgy* **62**, 2001, pp. 31-39
- [12] *A.M.S. Oancea, M. Radulescu, D. Oancea, E. Pincovschi*, Three Generations of Polystyrene-Type Strong Acid Cation Exchangers: Textural Effects on Proton/Cadmium(II) Ion Exchange Kinetics, *Ind. Eng. Chem. Res.* **45**, 2006, pp. 9096-9106
- [13] *A.M.S. Oancea, A.R. Popescu, M. Radulescu, V. Weber, E. Pincovschi, M. Cox*, Kinetics of Cesium and Strontium Ions Removal from Wastewater on Gel and Macroporous Resins, *Solvent Extr. Ion. Exch.* **26**, 2008, pp. 217-239
- [14] *V. Weber and E. Pincovschi*, H^+ - K^+ Ion Exchange Kinetics on Weak Acid Resin, *U.P.B. Sci. Bull., Series B*, **70**, Iss. 4, 2008, pp. 57-66
- [15] *C.M. Bohdana, D.S. Cantea, J.A. Dale, E. Pincovschi and A.M.S. Oancea*, Polymeric Ion Exchangers Based on Styrene-Divinylbenzene Matrix. Textural and Structural Modifications after Grafting Different Functional Groups, in Recent Advances in Ion Exchange Theory and Practice, Proceedings IEX 2008, Editor M.Cox, Society of Chemical Industry (SCI), London, 2008, pp. 427-434
- [16] *D.R. Linde*, Editor, CRC Handbook of Chemistry and Physics, 85th edition 2005, CRC Press; Boca Raton, 2005, Section 5, Thermochemistry, Electrochemistry and Kinetics 5-91, Ionic Conductivity and Diffusion at Infinite Dilution, Table 5-93.
- [17] *F. Helfferich*, Ion Exchange Kinetics. III. Experimental Test of the Theory of Particle-Diffusion Controlled Ion-Exchange, *J. Phys. Chem.* **66**, 1962, pp. 39-44
- [18] *F. Helfferich*, Ion Exchange Kinetics. IV. Demonstration of the Dependence of the Interdiffusion Coefficient on Ionic Composition, *J. Phys. Chem.* **67**, 1963, pp. 1157-1159
- [19] *E.R. Nightingale, Jr.*, Phenomenological Theory of Ion Solvation. Effective Radii of Hydrated Ions, *J. Phys. Chem.* **63**, 1959, pp. 1381-1387.

[20] J.E. Hueey, E.A. Keiter, R.L. Keiter, *Chimie Inorganique*, De Boeck & Larcier s.a., 1996, Paris, pp. 114-117.